

# Towards 2- $\mu\text{m}$ comb light source based on multiple four-wave mixing in a dual-frequency Brillouin fiber laser

Moise Deroh<sup>1,2,\*</sup>, Gang Xu<sup>1,3</sup>, Erwan Lucas<sup>1</sup>, Jean-Charles Beugnot<sup>2</sup>, Hervé Maillotte<sup>2</sup>, Thibaut Sylvestre<sup>2</sup>, and Bertrand Kibler<sup>1</sup>

<sup>1</sup> Laboratoire Interdisciplinaire Carnot de Bourgogne, UMR 6303 CNRS, Université de Bourgogne, Dijon, France

<sup>2</sup> Institut FEMTO-ST, UMR 6174 CNRS, Université Franche-Comté, Besançon, France

<sup>3</sup> School of Optical and Electronic Information, Huazhong University of Science and Technology, Wuhan, P. R. China

\* Email: [koffi.deroh@u-bourgogne.fr](mailto:koffi.deroh@u-bourgogne.fr)

In this study, we report the generation of multi-wavelength light sources through enhanced four-wave-mixing processes using a straightforward and adaptable dual-frequency Brillouin fiber laser. This passive optical and nonreciprocal cavity is first tested and analyzed with long fiber lengths up to 1 km in the 1.55  $\mu\text{m}$  telecommunication C band and then in the 2- $\mu\text{m}$  waveband. In the latter case, we demonstrate that our fiber cavity enables efficient multiple four-wave mixings, in the continuous-wave regime, which are commonly inaccessible in long silica-fibers due to increased losses. We also report on the tunable repetition rate from tens of GHz to hundreds of GHz, by simply changing the frequency spacing between the two continuous-wave pumps. The coherence limitations of our all-fiber system are discussed, along with the impact of the dispersion regime of the nonlinear fiber that forms the cavity.

**Keywords:** Stimulated Brillouin scattering, fiber cavities, four-wave mixing, frequency combs.

## 1. INTRODUCTION

Compact and coherent comb light sources in the 2- $\mu\text{m}$  waveband are becoming attractive components for molecular spectroscopy, environmental monitoring, and next-generation high-speed optical communications [1–6]. Coherent comb light sources can be obtained in general through various optical configurations such as electro-optic modulation schemes and mode-locked pulsed lasers often assisted by additional nonlinear frequency conversion [7–11], and parametric oscillations from a continuous-wave (CW) laser in high quality factor microresonators [12–13]. Mostly, developed systems focused on the telecommunication wavelength around 1.55  $\mu\text{m}$ , thus benefiting from the numerous high-quality optical components. In the specific 2- $\mu\text{m}$  waveband, common approaches typically involve near-infrared to mid-infrared conversion techniques of frequency combs and mode-locked lasers [14–15]. Alternately, other systems may be implemented using thulium (Tm)-doped silica fiber lasers and components or semiconductor lasers [2–3]. It is also worth mentioning that multi-wavelength fiber lasers have been developed around 2  $\mu\text{m}$  using distinct cavity arrangements based on Tm-doped fibers [16–20].

In general, direct generation of comb light sources in the 2- $\mu\text{m}$  waveband remains challenging in a cavity-free configuration with CW pumping, for instance, due to the detrimental losses in the required long optical fiber lengths (typically, tens of dB/km). As a consequence, multiple four-wave mixing (MFWM) processes in the simultaneous propagation of two pump waves through an optical fiber cannot be simply applied as in the conventional telecommunication window [21], even if bi-chromatic pumping allows for FWM to be free of power threshold. However, another alternative for generating combs has recently

41 emerged by combining Kerr and Brillouin effects with the aim of improving some nonlinear performances.  
42 Indeed, stimulated Brillouin scattering (SBS) can manifest with several orders of magnitude stronger than  
43 the Raman or Kerr effect, and it is also tunable over a wide spectral range [22]. Then one can excite and  
44 enhance MFWM processes in a non-reciprocal fiber cavity platform featuring bichromatic Brillouin lasing  
45 [23]. Direct coherent pumping is replaced by lasing on specific cavity modes, offering easily adjustable  
46 repetition rates and enhanced coherence by Brillouin purification [24]. A similar approach can be applied  
47 for generating a Kerr comb in an optical microresonator, using the Brillouin laser generated in the same  
48 cavity [25]. Highly coherent combs were also demonstrated in short fiber cavities by finely controlling the  
49 bi-chromatic Brillouin lasing [24].

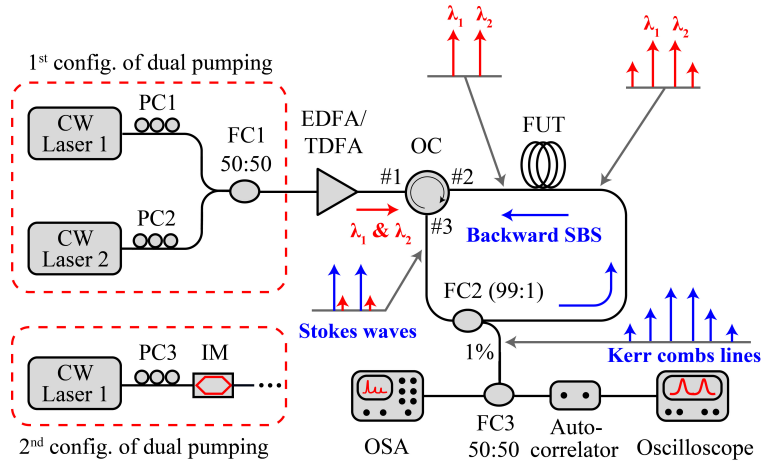
50 In this paper, we investigate two multi-line fiber laser sources centered at 1.55  $\mu\text{m}$  (C-band) and 2- $\mu\text{m}$   
51 (thulium band) that exhibit a symmetrical spectral comb structure based on enhanced MFWM within a  
52 long passive fiber cavity platform, specifically designed for bi-chromatic Brillouin lasing. At 1.55  $\mu\text{m}$ , we  
53 generated a multi-wavelength light source that operates in both dispersion regimes with distinct temporal  
54 and spectral features. Temporal characterization of the generated pulse train is provided by means of  
55 intensity autocorrelation measurements. Finally, at 2  $\mu\text{m}$ , we demonstrate a multi-wavelength light source  
56 made of 22 comb lines operating in the anomalous dispersion regime with a frequency spacing up to 106  
57 GHz. The stability and coherence of the multi-line sources and generated pulse trains are also discussed  
58 for the two pumping configurations.

59

## 60 **2. EXPERIMENTAL SETUP**

61 In our experiments, we analyzed two distinct cavities made of commercially available highly nonlinear  
62 fibers (HNLF) that exhibit a normal and anomalous dispersion. The main physical parameters of both  
63 cavities are summarized in Table 1 below. Figure 1 shows the experimental setup used for generating our  
64 multi-wavelength sources in both spectral bands, namely 1.55 and 2  $\mu\text{m}$ . The bi-chromatic pumping  
65 configuration can be achieved by combining two wavelength-tunable CW lasers (external cavity laser  
66 diodes) or by means of electro-optical (intensity) modulation (EOM) of one laser, to vary the pump  
67 frequency spacing [24]. Here, we chose two CW lasers to investigate larger frequency spacings. The two  
68 pump lasers were amplified via an erbium or thulium-doped fiber amplifier (EDFA/TDFA) and then injected  
69 into the passive fiber cavity via an optical circulator (OC). The backscattered Brillouin signals coming back  
70 from the FUT, shifted at the Brillouin frequency around 9.6 GHz [24] and 7.5 GHz [26] at 1.55 and 2  $\mu\text{m}$ ,  
71 respectively from our HNLF fibers, are then reinjected into the cavity ring via a fiber coupler (99:1). The  
72 output of the dual-frequency Brillouin fiber laser is extracted from a 1 % fiber coupler while the remaining  
73 99 % is fed back into the ring cavity. An OC closes the ring cavity. This configuration system allows free  
74 propagation of the Stokes waves, which perform multiple roundtrips in the counterclockwise direction  
75 (dual lasing occurs and initiates a cascade of FWM), while the pumps waves interact only over a single pass  
76 in the clockwise direction. We finally analyzed the output cavity spectrum using an optical spectrum  
77 analyzer (with 0.08 pm and 0.05 nm resolution, at 1.55 and 2  $\mu\text{m}$  respectively) and a rapid scanning  
78 intensity autocorrelator. In order to maximize the efficiency of the cascaded FWM processes, polarization  
79 controllers are inserted between the pumping lasers and the couplers to ensure that the two pumps have  
80 the same polarization direction. Specific fiber components dedicated to the 1.55 or 2- $\mu\text{m}$  spectral bands  
81 can be easily interchanged.

82



83 **Fig. 1.** Experimental setup for generating multi-wavelength light sources at both 1.55  $\mu\text{m}$  and 2  $\mu\text{m}$  by means of MFWM  
 84 in a dual-frequency Brillouin fiber laser. CW: Continuous wave, PC: Polarization Controller, IM: Intensity Modulator, FC:  
 85 Fiber Coupler, EDFA/TDFA: Erbium/Thulium Doped Fiber Amplifier, OC: Optical Circulator, FUT: Fiber Under Test,  
 86 OSA: Optical Spectrum Analyzer.

87

88 **Table 1:** Physical parameters at 1550 nm of the cavities study made of two distinct HNLFs in this work.

Fiber cavity parameters	Cavity 1	Cavity 2	Units
Cavity length (L)	350	1000	m
Brillouin gain efficiency ( $g_B/A_{eff}$ )	0.38	0.38	$\text{m}^{-1}.\text{W}^{-1}$
Brillouin gain bandwidth ( $\Delta\nu_B$ )	55	55	MHz
Total roundtrip loss	1.5	2.2	dB
Zero dispersion wavelength ( $\lambda_0$ )	1575	1523	nm
Dispersion parameter (D)	-2.95	0.49	$\text{ps}.\text{nm}^{-1}.\text{km}^{-1}$
Group-velocity dispersion ( $\beta_2$ )	3.77	-0.62	$\text{ps}^2.\text{km}^{-1}$
Nonlinear coefficient ( $\gamma$ )	12.5	10	$\text{W}^{-1}.\text{km}^{-1}$
Free spectral range (FSR)	0.6	0.22	MHz
Cavity finesse	8.69	5.94	-

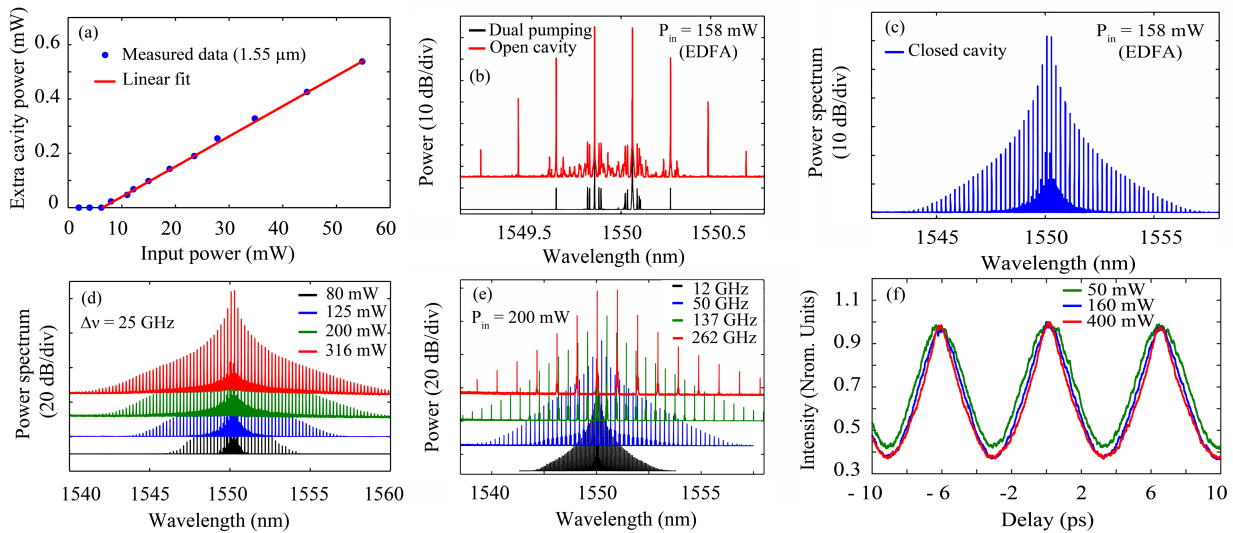
89

### 90 3. EXPERIMENTAL RESULTS AT 1.55 $\mu\text{m}$

91 In the following, our experiments were first performed at 1.55  $\mu\text{m}$  with the first cavity made of the  
 92 normally-dispersive HNLF. We first measured the output dual-frequency Brillouin laser power as a function  
 93 of injected pump power, as shown in Fig. 2 (a), and for a given frequency spacing of 25 GHz. A low lasing  
 94 threshold of 7.5 mW was experimentally achieved. For a 25-GHz (0.2 nm) frequency spacing and 158-mW  
 95 pump power, we specifically show the multi-line spectrum that was obtained in both open and closed  
 96 cavity configurations as depicted in Figs. 2 (b-c). Note that FWM processes occur and are analyzed in the  
 97 clockwise direction in the particular open-cavity configuration, since there is no Brillouin Stokes lasing. The  
 98 enhanced efficiency of the cascaded FWM process in a closed cavity is evident when driven by the Brillouin  
 99 Stokes. This results in a notable increase, transitioning from a limited number of comb lines to a substantial  
 100 expansion, reaching dozens. Figure 2(d) shows the resulting spectral evolution by increasing the injected  
 101 pump power from 80 to 316 mW in the closed cavity case. The number of comb lines increases

102 significantly; however, the overall spectral shape exhibits an exponential decay when the pump power  
 103 increases. This rapid decline in power per line can be attributed to both the strong normal cavity dispersion  
 104 and also the multimode Brillouin lasing regime for such long cavity length and high operating power [24].  
 105 Operating the Stokes lasers in the multimode regime leads to a strong degradation in comb coherence as  
 106 the Stokes pumps fluctuate across several cavity modes. Moreover, the thermal drift of our cavity relative  
 107 to the pump lasers is not counterbalanced by any phase-lock loop, contrary to our previous work on a very  
 108 short cavity [24]. As a result, our measurements only reflect a strong averaging of spectral broadening in  
 109 the presence of pump power and cavity detuning fluctuations. Nevertheless, we show that the generated  
 110 comb source can be tuned over a few hundreds of GHz by simply modifying the initial frequency spacing  
 111 of the two CW pumps. We measured the dependence of the output cavity spectrum as a function of the  
 112 frequency spacing for a given input power of 200 mW in Fig. 2(e). More particularly, we increased the  
 113 pump frequency spacing from 12.5 to 262 GHz (0.1 - 2.1 nm). The spectral bandwidth of the generated  
 114 comb lines exhibits rapid expansion up to a saturation point, accompanied by a decrease in the number of  
 115 lines. This behavior is attributed to the inherent dispersion of the fiber, which restricts the spectral  
 116 broadening, or, in other words, the maximum steepening of the temporal pulse fronts originating from  
 117 the initial sinusoidal modulation induced by the two pumps [27]. Indeed, we characterized the temporal  
 118 properties of the multi-wavelength spectrum with frequency spacing of 150 GHz for distinct pump powers,  
 119 by means of a second-harmonic autocorrelator with a resolution of 10 fs (see Fig. 2(f)). Under normal  
 120 cavity dispersion, the initial sinusoidal temporal pattern resulting from the interference of the two Stokes  
 121 fields in the cavity becomes a near-rectangular pulse train for increasing powers associated with larger  
 122 spectral broadenings, as confirmed by the triangular waveform of the autocorrelation profile with a period  
 123 of 6.7 ps.

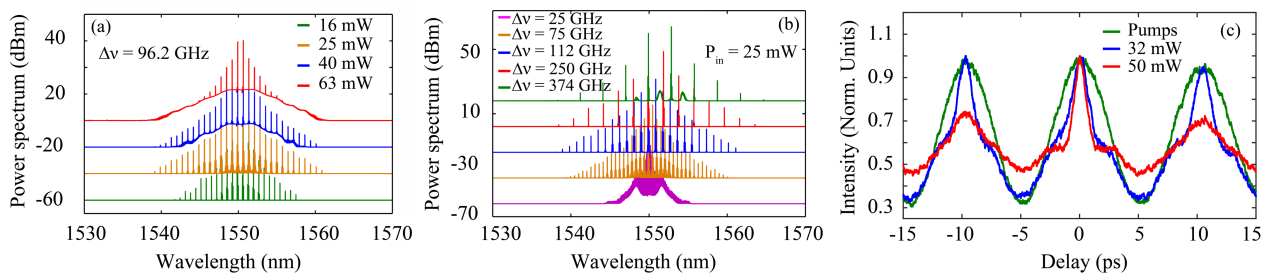
124



125

126 **Fig. 2.** Dual-frequency Brillouin laser and multi-wavelength light generation (cavity 1, normal dispersion regime). (a)  
 127 Stokes lasing threshold measurement. (b) Experimental FWM results for bi-chromatic pumping (25-GHz frequency  
 128 spacing) of the HNLf and cavity-free configuration for an input power of 158 mW. (c) Corresponding multi-wavelength  
 129 generation in the closed cavity configuration. (d) Spectral broadening recorded (25-GHz frequency spacing) at  
 130 increasing input pump powers from 80 to 316 mW. (e) Tunable frequency spacing of the multi-wavelength source for  
 131 an input power of 200 mW. (f) Experimental autocorrelation traces of the generated pulse train with a period of 6.7 ps  
 132 (repetition rate of 150 GHz) for distinct input powers of 50 to 400 mW.

133 Next, we carried out experiments with the second cavity made of the 1-km-long HNLF operating in the  
 134 anomalous dispersion. We measured the spectral evolution of the output cavity for a given frequency  
 135 spacing of 96.2 GHz (0.77 nm) and increased input powers from 16 to 63 mW (see Fig. 3(a)). In this  
 136 dispersion regime, we once again observe the generation of a multi-wavelength light source; however, the  
 137 spectral broadening experiences swift saturation at moderate powers, typically above 25 mW.  
 138 Subsequently, a pronounced increase in the noise background becomes evident, creating a substantial  
 139 pedestal beneath the comb lines. This distinct characteristic of the anomalous dispersion regime is closely  
 140 related to the growth of modulation instability (MI) sidelobes. This adverse phenomenon, detrimental to  
 141 coherence properties, was also observed in short fiber cavities [27]. However, it was successfully mitigated  
 142 by employing suitable detuning conditions, resulting in the formation of a globally coherent comb. By  
 143 contrast, the MI here prevents the growth of the combs lines in our long free-running cavity. In this case,  
 144 it is important to avoid the MI effect. To this end, we restricted the input power to values below 25 mW.  
 145 We then noticed that the MI emergence also depends on the frequency spacing between the two pumps.  
 146 Figure 3(b) shows the output spectra obtained with different frequency spacings for an input power of  
 147 25 mW. We significantly increased the pump frequency spacing from 25 to 373.9 GHz (0.2 - 3.0 nm). We  
 148 clearly confirm that the comb repetition rate can be easily tuned over a few hundreds of GHz. However,  
 149 we note that MI sidelobes appear only for small or large frequency spacings (below 75 GHz or beyond  
 150 250 GHz). For a small frequency spacing, MI amplifies the noise under the overall MFWM spectrum, while  
 151 MI sidelobes emerge between comb lines for a large frequency detuning. In between, when the pump  
 152 frequency spacing is close to the MI offset frequency, the detrimental impact of MI remains negligible, at  
 153 least for such a power. Indeed, in Fig. 3(c), we provide the temporal autocorrelation traces of the multi-  
 154 wavelength source generated with 96.2-GHz frequency spacing (0.77 nm) for several pump powers. We  
 155 found that the initial sinusoidal pattern with a period of 10.4 ps evolves into a nearly triangular pattern  
 156 with increasing powers (i.e. associated with larger spectra). However, for an input power of 32 mw, we  
 157 clearly distinguish the formation of a localized short temporal structure within each period of the initial  
 158 beating, in contrast with the normal dispersion regime. However, at input powers exceeding 50 mW, a  
 159 noticeable decline in the intensity coherence of the temporal pattern is observed, directly attributed to  
 160 the detrimental impact of MI, as depicted in Fig. 3(a). The reduced contrast between the central  
 161 autocorrelation peak and the neighboring intercorrelation peaks in the signal exposes a pronounced jitter  
 162 in the pulse train, related to coherence loss of the multi-line comb source.



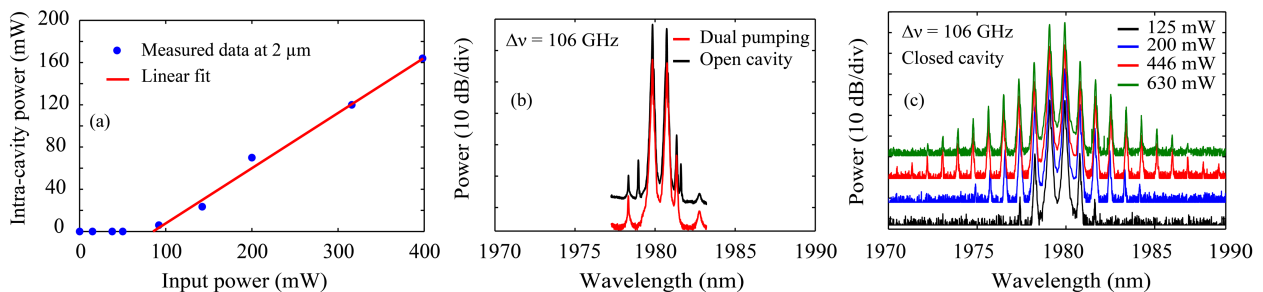
163  
 164 Fig. 3. Dual-frequency Brillouin laser and multi-wavelength light generation (cavity 2, anomalous dispersion regime). (a)  
 165 Experimental FWM results for bi-chromatic pumping (96.2 GHz frequency spacing) of the HNLF and increasing input  
 166 powers from 16 to 63 mW. (b) Tunable frequency spacing (from 25 GHz to 374 GHz) of the multi-wavelength source

167 for an input power of 25 mW. (c) Experimental autocorrelation traces of the generated pulse train with a period of 10.4 ps  
 168 (rep. rate of 96.2 GHz) for input powers of 32 to 50 mW.

169 **4. EXPERIMENTAL RESULTS AT 2  $\mu\text{m}$**

170 Thanks to the simple architecture of our system, we extended this work to the 2- $\mu\text{m}$  waveband by  
 171 interchanging suitable fiber components and pump lasers. Due to the high linear losses of silica-based  
 172 fibers in this spectral range, we used the shorter normally-dispersive HNLf (length equal to 350 m), which  
 173 still exhibits normal dispersion ( $\beta_2 \sim 1\text{ps}^2/\text{km}$ ) around 1.95-2.0  $\mu\text{m}$ . We first measured the dual-frequency  
 174 Brillouin lasing threshold by extracting only 1 % of the optical cavity power as a function of the injected  
 175 pump power. As shown in Fig. 4(a), an input power of 90 mW allowed us to reach the dual-frequency  
 176 Stokes lasing in our ring cavity in the case of a frequency spacing of 106 GHz (0.85 nm) around 1.98  $\mu\text{m}$ . In  
 177 Figure 4(b), the experimental spectrum of the initial dual-frequency pumping is illustrated alongside the  
 178 corresponding output of the HNLf fiber (i.e., open cavity configuration) for an input power of 200 mW.  
 179 Because of the higher fiber losses at such wavelengths (about 15 dB/km), the cascaded FWM process  
 180 proves to be highly inefficient in this cavity-free configuration, failing to generate any new spectral lines.  
 181 This outcome persists despite the judicious selection of this fiber due to its moderate losses compared to  
 182 typical silica fibers. It becomes here obvious that our closed cavity configuration based on the dual-  
 183 frequency Brillouin laser will provide an interesting solution for MFWM processes and the generation of a  
 184 multi-wavelength light source. Figure 4(c) confirms this claim by showing the spectral broadening obtained  
 185 in the cavity upon increasing input powers from 125 mW to 630 mW. As previously shown, the cavity  
 186 operating in the normal dispersion does not present any saturation of MFWM due to MI. The number of  
 187 comb lines increases rapidly to 22 lines when the input power reaches 446 mW. Furthermore, within this  
 188 specific range of a few hundred milliwatts, we observe a spectral saturation, mirroring the behavior  
 189 observed in the 1.55- $\mu\text{m}$  experiment. It is important to note that the generated comb lines are fewer in  
 190 number compared to those at 1.55  $\mu\text{m}$ , primarily due to the higher cavity losses, exhibiting an order of  
 191 magnitude difference.

192



193

194 Fig. 4. Dual-frequency Brillouin lasing and comb source generation in a multimode regime at a wavelength of 2  $\mu\text{m}$   
 195 wavelength. (a) Stokes laser threshold measurement. (b) Experimental recording with 106 GHz frequency spacing of  
 196 the dual pumping and cavity-free FWM configuration at 200 mW pump power. (c) Brillouin/Kerr multiwavelength lines  
 197 dynamics as a function of the injected power at fixed pumps frequency of 106 GHz in close cavity configuration.

198

199

200 **5. CONCLUSION**

201 In conclusion, despite the utilization of extended cavity lengths in the dual-frequency Brillouin fiber laser  
202 leading to a multimodal laser operation, we experimentally verified the efficient generation of  
203 multiwavelength sources through cascaded four-wave mixing processes at both 1.55  $\mu\text{m}$  (C-band) and 2  
204  $\mu\text{m}$  (thulium band). The number of comb lines rapidly increases with input power, and their frequency  
205 spacing can be tuned by varying the initial pump wavelengths. Distinct features related to the sign of net  
206 cavity dispersion are also revealed. This long-cavity configuration was previously explored in Ref. [23] at  
207 1.55  $\mu\text{m}$  but in only one dispersion regime, without highlighting the detrimental impact of MI.

208 Additionally, we extend the approach to the 2- $\mu\text{m}$  waveband, where MFWM in the continuous-wave  
209 regime is typically inaccessible due to strong fiber losses. No asymmetric spectral broadenings were  
210 observed when initial power is equally distributed over the two pumps, since we are operating in a free-  
211 running configuration without a phase-locking loop scheme (in contrast with Ref. [24], where pump  
212 detuning is effectively controlled). Nevertheless, the enhanced performances of MFWM in this simple  
213 architecture of the Brillouin fiber laser make it readily applicable at any wavelength where fiber  
214 components and CW lasers are available. A simple future application could also concern not only the mid-  
215 infrared region but also the high-demanding 1- $\mu\text{m}$  waveband. However, to preserve the full coherence  
216 properties of the generated combs, one has to implement a stabilization scheme as recently demonstrated  
217 at 1  $\mu\text{m}$  [28].

218

## 219 6. REFERENCE LIST

220

- 221 1. K. C. Cossel, E. M. Waxman, I. A. Finneran, G. A. Blake, J. Ye, and N. R. Newbury, "Gas-phase  
222 broadband spectroscopy using active sources: progress, status, and applications [Invited]," *J. Opt.*  
223 *Soc. Am. B* **34**, 104-129 (2017).
- 224 2. E. Russell, B. Corbett, and F. C. Garcia Gunning, "Gain-switched dual frequency comb at 2  $\mu\text{m}$ ," *Opt.*  
225 *Express* **30**, 5213-5221 (2022).
- 226 3. A. Parriaux, K. Hammani, and G. Millot, Two-micron all-fibered dual-comb spectrometer based on  
227 electro-optic modulators and wavelength conversion. *Commun Phys* **1**, 17 (2018).
- 228 4. W. Cao, D. Hagan, D. J. Thomson, M. Nedeljkovic, C. G. Littlejohns, A. Knights, S.-U. Alam, J. Wang, F.  
229 Gardes, W. Zhang, S. Liu, K. Li, M. S. Rouified, G. Xin, W. Wang, H. Wang, G. T. Reed, and G. Z.  
230 Mashanovich, "High-speed silicon modulators for the 2  $\mu\text{m}$  wavelength band," *Optica* **5**, 1055–1062  
231 (2018).
- 232 5. F. Gunning and B. Corbett, "Time to open the 2- $\mu\text{m}$  window?" *Opt. Photon. News* **30**, 42–47 (2019).
- 233 6. A. C. Dada, J. Kaniewski, C. Gawith, M. Lavery, R. H. Hadfield, D. Faccio, and M. Clerici, "Near-Maximal  
234 Two-Photon Entanglement for Optical Quantum Communication at 2.1 $\mu\text{m}$ ," *Phys. Rev. Appl.* **16**,  
235 L051005 (2021).
- 236 7. A. Parriaux, K. Hammani, and G. Millot, "Electro-optic frequency combs," *Adv. Opt. Photon.* **12**, 223-  
237 287 (2020).
- 238 8. M. I. Kayes and M. Rochette, "Optical frequency comb generation with ultra-narrow spectral lines,"  
239 *Opt. Lett.* **42**, 2718–2721 (2017).



- 240 9. R. Wu, V. R. Supradeepa, C. M. Long, D. E. Leaird, and A. M. Weiner, "Generation of very flat optical  
241 frequency combs from continuous-wave lasers using cascaded intensity and phase modulators  
242 driven by tailored radio frequency waveforms," *Opt. Lett.* **35**, 3234–3236 (2010).
- 243 10. B. R. Washburn, S. A. Diddams, N. R. Newbury, J. W. Nicholson, M. F. Yan, and C. G. Jørgensen,  
244 "Phase-locked, erbium-fiber-laser-based frequency comb in the near infrared," *Opt. Lett.* **29**, 250–  
245 252 (2004).
- 246 11. S. T. Cundiff and J. Ye, "Colloquium: Femtosecond optical frequency combs," *Rev. Mod. Phys.* **75**,  
247 325 (2003).
- 248 12. P. Del’Haye, A. Schliesser, O. Arcizet, T. Wilken, R. Holzwarth, and T. J. Kippenberg, "Optical  
249 frequency comb generation from a monolithic microresonator", *Nature* **450**, 1214-1217 (2007).
- 250 13. T. J. Kippenberg, R. Holzwarth, and S. A. Diddams, "Microresonator-Based Optical Frequency Combs,"  
251 *Science* **332**, 555-559 (2013).
- 252 14. S. Xing, A. S. Kowligy, D. M. B. Lesko, A. J. Lind, and S. A. Diddams, "All-fiber frequency comb at 2  $\mu\text{m}$   
253 providing 1.4-cycle pulses," *Opt. Lett.* **45**, 2660-2663 (2020).
- 254 15. X. Wang, K. Jia, M. Chen, S. Cheng, X. Ni, J. Guo, Y. Li, H. Liu, L. Hao, J. Ning, G. Zhao, X. Lv, S.-W.  
255 Huang, Z. Xie, and S.-N. Zhu, "2  $\mu\text{m}$  optical frequency comb generation via optical parametric  
256 oscillation from a lithium niobate optical superlattice box resonator," *Photon. Res.* **10**, 509-515  
257 (2022).
- 258 16. K. Hu, I. V. Kabakova, S. Lefrancois, D. D. Hudson, S. He, and B. J. Eggleton, "Hybrid Brillouin/thulium  
259 multiwavelength fiber laser with switchable single- and double-Brillouin-frequency spacing," *Opt.*  
260 *Express* **22**, 31884–31892 (2014).
- 261 17. S. Zhao, P. Lu, D. Liu, and J. Zhang, "Switchable multiwavelength thulium-doped fiber ring lasers,"  
262 *Opt. Eng.* **52**, 086105 (2013).
- 263 18. X. Wang, Y. Zhu, P. Zhou, X. Wang, H. Xiao, and L. Si, "Tunable, multiwavelength Tm-doped fiber laser  
264 based on polarization rotation and four-wave-mixing effect," *Opt. Express* **21**, 25977–25984 (2013).
- 265 19. W. Peng, F. Yan, Q. Li, S. Liu, T. Feng, and S. Tan, "A 1.97  $\mu\text{m}$  multiwavelength thulium-doped silica  
266 fiber laser based on a nonlinear amplifier loop mirror," *Laser Phys. Lett.* **10**, 115102 (2013).
- 267 20. Shuisen Jiang, Changlei Guo, Hongyan Fu, Kaijun Che, Huiying Xu, and Zhiping Cai, "Mid-infrared  
268 Raman lasers and Kerr-frequency combs from an all-silica narrow-linewidth microresonator/fiber  
269 laser system," *Opt. Express* **28**, 38304-38316 (2020).
- 270 21. J. Fatome, S. Pitois, C. Fortier, B. Kibler, C. Finot, G. Millot, C. Courde, M. Lintz, and E. Samain,  
271 "Multiple four-wave mixing in optical fibers: 1.5–3.4-THz femtosecond pulse sources and real-time  
272 monitoring of a 20-GHz picosecond source," *Opt. Commun.* **283**, 2425–2429 (2010).
- 273 22. C. Wolff, M. J. A. Smith, B. Stiller, and C. G. Poulton, "Brillouin scattering—theory and experiment:  
274 tutorial," *J. Opt. Soc. Am. B* **38**, 1243-1269 (2021).
- 275 23. Q. Li, Z. Jia, Z. Li, Y. Yang, J. Xiao, S. Chen, G. Qin, Y. Huang, and W. Qin, "Optical frequency combs  
276 generated by four-wave mixing in a dual wavelength Brillouin laser cavity," *AIP Adv.* **7**, 075215  
277 (2017).
- 278 24. E. Lucas, M. Deroh, and B. Kibler, "Dynamic Interplay Between Kerr Combs and Brillouin Lasing in  
279 Fiber Cavities," *Laser Photonics Rev.* **17**, 2300041 (2023).
- 280 25. Y. Bai, M. Zhang, Q. Shi, S. Ding, Y. Qin, Z. Xie, X. Jiang, and M. Xiao, "Brillouin-Kerr Soliton Frequency  
281 Combs in an Optical Microresonator," *Phys. Rev. Lett.* **126**, 063901 (2021).



- 282 26. M. Deroh, J.-C. Beugnot, K. Hammani, C. Finot, J. Fatome, F. Smektala, H. Maillotte, T. Sylvestre, and  
283 B. Kibler, "Comparative analysis of stimulated Brillouin scattering at 2  $\mu\text{m}$  in various infrared glass-  
284 based optical fibers," *J. Opt. Soc. Am. B* **37**, 3792–3800 (2020).
- 285 27. M. Deroh, E. Lucas, and B. Kibler, " Dispersion engineering in a Brillouin fiber laser cavity for Kerr  
286 frequency comb formation," *Opt. Lett* **48**, 6388–6391 (2023).
- 287 28. M. Deroh, E. Lucas, K. Hammani, G. Millot, and B. Kibler, " Stabilized single-frequency sub-kHz  
288 linewidth Brillouin fiber laser cavity operating at 1  $\mu\text{m}$ ," *Appl. Opt.* **62**, 8109–8114 (2023).
- 289